Tetrahedron 66 (2010) 1915–1924

Contents lists available at ScienceDirect

Tetrahedron

journal homepage: www.elsevier.com/locate/tet

Mechanistic comparison of aluminium based catalysts for asymmetric cyanohydrin synthesis

Michael North *, Pedro Villuendas, Courtney Williamson

School of Chemistry and University Research Centre in Catalysis and Intensified Processing, Bedson Building, Newcastle University, Newcastle upon Tyne. NE1 7RU, UK

ARTICLE INFO

Article history:
Received 18 September 2009
Received in revised form 27 November 2009
Accepted 4 January 2010
Available online 11 January 2010

Keywords:
Aluminium
Cyanohydrin
Kinetics
Phosphine oxide
Lewis acid
Lewis base

ABSTRACT

A kinetic analysis of the asymmetric addition of trimethylsilyl cyanide to benzaldehyde using three aluminium based catalysts has been carried out. All three catalysts displayed rate equations, which were first order in trimethylsilyl cyanide concentration and zero order in benzaldehyde concentration. The results are consistent with a common mechanism for effective asymmetric catalysis of cyanohydrin synthesis, involving combined activation of the aldehyde by a Lewis acid and activation of the trimethylsilyl cyanide by a Lewis base. The mechanistic analysis was also applied to a magnesium-based catalyst system to demonstrate its general applicability.

1. Introduction

Over the last fifteen years there has been an explosion in interest in asymmetric cyanohydrin synthesis in which a chiral catalyst is used to induce the asymmetric addition of a cyanide source to aldehydes or ketones (Scheme 1). The chiral catalyst may be a metal derived Lewis acid,[1,2] a synthetic organocatalyst,[2–4] or an enzyme.[5] Some of these processes have been commercialized for the synthesis of α-hydroxyacids and β-aminoalcohols.[5–7]

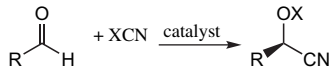

Scheme 1. Catalytic asymmetric cyanohydrin synthesis.

Whilst the mechanism of achiral cyanohydrin synthesis using basified hydrogen cyanide was elucidated by Lapworth over a century ago,[8–11] the mechanisms involved in asymmetric cyanohydrin synthesis are more complex. Catalysts have been developed which incorporate Lewis acidic and/or Lewis basic functionalities and which will transfer cyanide from a wide range of cyanide sources including: metal cyanides, trimethylsilyl cyanide, acyl cyanides, cyanoformates, cyanophosphonates and other cyanohydrins.[1–4] Many authors have studied or speculated on the mechanism of action of a particular catalyst with a particular cyanide source,[1–4] however there has been no attempt to study the reaction more generally. Such an investigation might reveal the relative importance of acidic versus basic catalysis, activation of the carbonyl versus activation of cyanide, and ultimately result in a generally applicable mechanism or mechanisms, which are valid for all catalysts and cyanide sources. In this manuscript, we report the results of a kinetic study of three different, aluminium based, catalysts for the asymmetric addition of trimethylsilyl cyanide to aldehydes.

2. Kinetics

Catalysts **1**–**3** were chosen for this study. Each of these aluminium complexes can be prepared by a relatively short synthesis, requires the presence of an external phosphine oxide for optimal activity and is known to catalyse the asymmetric addition of trimethylsilyl cyanide to benzaldehyde, which was chosen as the test reaction. Thus, these three catalysts would allow the influence of both the Lewis acid and the Lewis/Brønsted base on the reaction mechanism to be probed. Whilst complexes **1**–**3** all have the same Lewis acidic metal, they differ with respect to the internal base. Complex **1**, which was developed by Shibasaki,[12,13] possesses pendant phosphine oxides, which have been proposed to act as Lewis bases and to activate the trimethylsilyl cyanide. The utility of complex **1** has been shown by its use in a number of total syntheses.[14–17]

Najera's catalyst **2**, retains the same axially chiral binol unit as complex **1**, but the pendant phosphine oxides are replaced by

* Corresponding author. Tel.: +44 191 222 7128; fax: +44 191 222 6929.
E-mail address: michael.north@ncl.ac.uk (M. North).

0040-4020/$ – see front matter © 2010 Elsevier Ltd. All rights reserved.
doi:10.1016/j.tet.2010.01.004

tertiary amines, which are proposed to act as Brønsted bases to activate and pre-organise hydrogen cyanide formed in situ from trimethylsilyl cyanide and water from molecular sieves added to the reaction mixture.[18,19] The versatility of complex **2** has been demonstrated by its ability to catalyse asymmetric cyanohydrin synthesis from a wide range of different cyanide sources.[20–26] A closely related catalyst in which the diethylamino groups of complex **2** are changed to morpholino groups has also been shown to catalyse the asymmetric addition of trimethylsilyl cyanide to aldehydes in the presence of a phosphine oxide additive.[27,28]

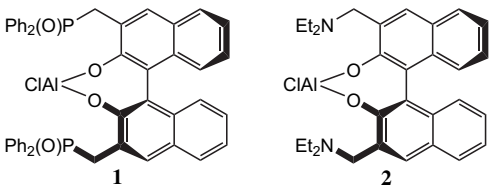

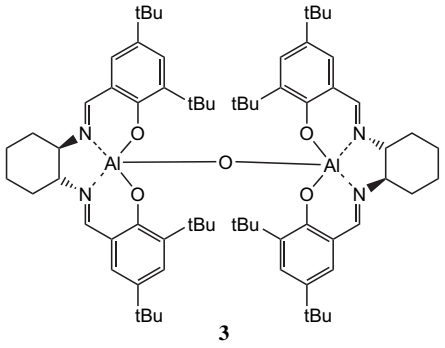

Complex **3** whose catalytic activity was recently reported by our group[29] does not possess any pendant basic features, but still requires the presence of triphenylphosphine oxide as a co-catalyst. A number of related monometallic aluminium(salen) complexes have also been shown to catalyse the asymmetric addition of trimethylsilyl cyanide to aldehydes and ketones, but in each case a phosphine oxide[30–33] or *N*-oxide[34,35] co-catalyst is required. Aluminium(salen)alkoxides have also been found to be effective asymmetric catalysts for the addition of cyanoformates to acylsilanes, leading to cyanohydrin trimethylsilyl ethers after a 1,2-Brook rearrangement.[36,37] In this case no phosphine oxide co-catalyst was required, but it was shown that the alkoxide could perform a similar role, liberating cyanide from the cyanoformate.

Catalyst **3** was prepared by the route we have previously reported.[38] Catalysts **1** and **2** are generated in situ from the binol ligand and dimethylaluminium chloride.[12–26] The binol ligand needed for the preparation of complex **1** was prepared as previously reported by Shibasaki,[12,13] however, for the synthesis of the ligand (BINOLAM) needed for the formation of Najera's catalyst **2**, we developed a three-step synthesis (Scheme 2) based on a bis-anionic Fries rearrangement reported by Dennis and Woodward.[39] Thus, reaction of (*R*)-binol with *N*,*N*-diethylcarbamoyl chloride gave bis-urethane **4**, which on treatment with *s*-BuLi followed by acidic work-up gave bis-amide **5**. Reduction of amide **5** with lithium aluminiumhydride gave BINOLAM **6** in 47% overall yield.

Catalysts **1**-**3** were first tested for the asymmetric addition of trimethylsilyl cyanide to benzaldehyde using conditions reported in the literature to confirm the efficacy of in situ prepared catalysts **1** and **2** (Table 1). The enantiomeric excess of the *O*-trimethylsilyl mandelonitrile **7** was determined by chiral GC analysis of *O*-acetyl mandelonitrile **8** prepared by the method of Kagan[40] (Scheme 3). In each case, the activity and enantioselectivity of the catalyst was comparable to that reported in the literature.

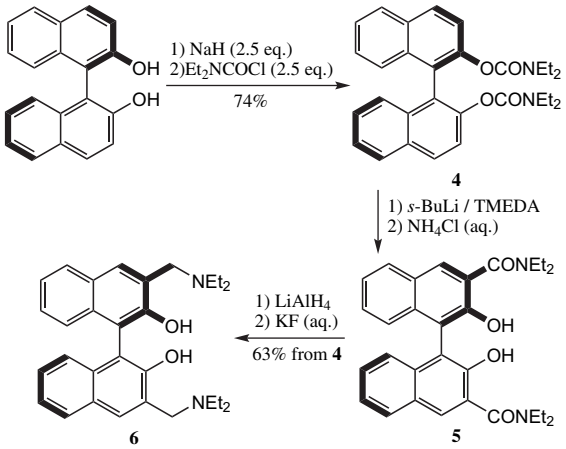

Scheme 2. Synthesis of BINOLAM.

Table 1
Synthesis of *O*-trimethylsilyl mandelonitrile using catalysts **1**–**3**

Catalyst (mol %)	Co-catalyst (mol %)	Solvent	Temp (°C)	Time (h)	Conversion (%)	Ee[a] (%)
1 (10)		CH_2Cl_2	−40	36	95 (91)[b]	83 (87)[b]
2 (10)[c]	Ph_3PO (40)	Toluene	−20	6	99 (99)[d]	>99.5 (>99.5)[d]
3 (2)	Ph_3PO (10)	CH_2Cl_2	−40	16	80[29]	89[29]
1 (10)	$MePh_2PO$ (40)	CH_2Cl_2	−40	96	93	69
1 (4)	$MePh_2PO$ (40)	CH_2Cl_2	0	16	16	15
1 (4)	$MePh_2PO$ (40)	CH_2Cl_2	20	2	75	4
1 (4)	$MePh_2PO$ (16)	CH_2Cl_2	20	2	68	3
2 (9)[c]	$MePh_2PO$ (40)	Toluene	−20	6	99	99
2 (9)[c]	$MePh_2PO$ (40)	Toluene	0	4	99	95
2 (2)[c]	$MePh_2PO$ (10)	Toluene	0	4	63	65
2 (2)	$MePh_2PO$ (10)	Toluene	0	4	49	60
2 (2)	$MePh_2PO$ (10)	Toluene	20	4	79	46
3 (1)	Ph_3PO (10)	CH_2Cl_2	−20	16	100[29]	80[29]
3 (1)	Ph_3PO (10)	CH_2Cl_2	0	6	100[29]	68[29]

[a] In all cases, the *S*-enantiomer of the cyanohydrin was obtained from the *R*-enantiomer of the catalyst.
[b] Values in brackets are those reported in the literature.[12,13]
[c] Reaction carried out in the presence of 4 Å molecular sieves.
[d] Values in brackets are those reported in the literature.[18,19]

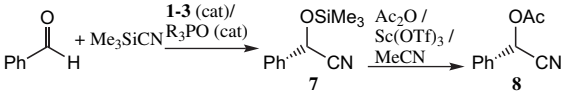

Scheme 3. Synthesis of (*S*)-mandelonitrile derivatives.

For catalyst **1**, the kinetics had to be monitored at −40 °C as at higher temperatures the enantioselectivity of the reactions was diminished to such an extent that it was not possible to be confident that a catalysed reaction was being monitored rather than racemic background reaction (Table 1). Whilst a reaction carried out in the absence of phosphine oxide went to 95% conversion in 36 h at −40 °C (Table 1), addition of methyldiphenylphosphine oxide significantly reduced the reaction rate but enhanced the enantioselectivity as previously reported by Shibasaki.[12,13] In the presence of methyldiphenylphosphine oxide, reactions typically required four days to go to completion. Never the less, kinetic experiments were carried out in the presence of methyldiphenylphosphine oxide, monitoring the reactions by ^1H NMR spectroscopy in CD_2Cl_2 since this allowed the kinetic influence of the Lewis base to be investigated. Shibasaki also reported[12,13] that slow addition of trimethylsilyl cyanide enhanced the enantioselectivity of reactions, but this was not compatible with our kinetic study, so all of the trimethylsilyl cyanide was added at the start of the reaction.

For catalyst **2** however, the standard conditions were heterogeneous due to the presence of 4 Å molecular sieves. To avoid this complication, variations to the reaction conditions were sought where the reaction would proceed in the absence of molecular sieves. In addition, the triphenylphosphine oxide was changed to methyldiphenylphosphine oxide to allow direct comparison with results obtained using Shibasaki's system. As can be seen from Table 1, changing the phosphine oxide had no effect on the reactivity or enantioselectivity of the catalyst system. Conducting the reaction at an experimentally more convenient 0 °C had only a slightly detrimental effect on the enantioselectivity in this case. Reducing the catalyst and phosphine oxide loadings to 2 mol % and 10 mol %, respectively did reduce both the yield and enantioselectivity, though these were still significant. Omission of the 4 Å molecular sieves at 0 °C reduced the rate of reaction still further, but had only a slightly detrimental effect on the enantioselectivity. Finally, reactions carried out at 20 °C proceeded to 79% conversion in 4 h, albeit with a reduced enantioselectivity of 46%. These conditions were adopted as the most convenient as they allowed reactions carried out in toluene-d_8 to be readily monitored by ^{1}H NMR spectroscopy as discussed above for the Shibasaki system.

For reactions catalysed by complex **3**, the standard conditions were too slow to allow convenient monitoring of the reaction kinetics. Therefore, the reaction temperature was increased. At the same time, the amount of catalyst **3** employed was decreased to prevent complications caused by the UV or NMR spectrum of the salen ligand interfering with the kinetic data. In this case however, triphenylphosphine oxide was retained as the Lewis base as alternatives were known to significantly reduce the reaction rate.[29] A reaction at −20 °C still required 16 h to go to completion, but at 0 °C reactions were complete in 6 h and the enantioselectivity (68%) was still acceptable. Under these conditions, the disappearance of benzaldehyde could be conveniently monitored from the UV absorbance at 246 nm of aliquots removed from the reaction mixture as we have previously reported for other metal(salen) complexes.[41–48]

Duplication of kinetics experiments showed that they gave rate data, which was reproducible within an error limit of ±6%. Having found reaction conditions under which the kinetics of asymmetric cyanohydrin synthesis catalysed by each of complexes **1–3** could be monitored, the complete rate equation for each catalyst system was determined by systematically varying the initial concentration of each component of the reaction. Reactions catalysed by each of complexes **1**–**3** were found to obey the same rate equation (Eq. 1) and to be first order in trimethylsilyl cyanide and zero order in benzaldehyde. The overall first order nature of the reactions is illustrated in Figure 1, and the dependence of the rate on the initial concentration of trimethylsilyl cyanide is shown for each catalyst in Figure 2. Experiments carried out at different initial concentrations of benzaldehyde confirmed that for each of catalysts **1**–**3**, the rate was independent of the benzaldehyde concentration.

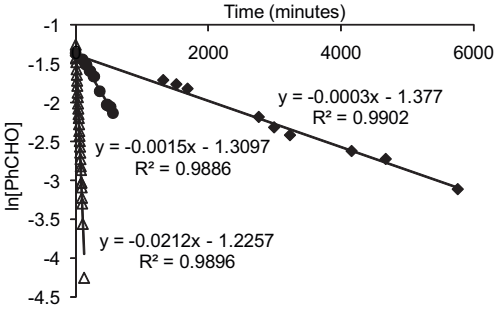

Figure 1. First order kinetics plots for catalysts **1**–**3**. Catalyst **1**: filled diamonds ([PhCHO]$_0$=0.25 M, [Me$_3$SiCN]$_0$=0.42 M, [**1**]=0.025 M, [MePh$_2$PO]=0.093 M). Catalyst **2**: unfilled triangles ([PhCHO]$_0$=0.26 M, [Me$_3$SiCN]$_0$=0.39 M, [**2**]=0.005 M, [MePh$_2$PO]=0.035 M). Catalyst **3**: filled circles ([PhCHO]$_0$=0.25 M, [Me$_3$SiCN]$_0$=0.40 M, [**3**]=0.005 M, [Ph$_3$PO]=0.025 M).

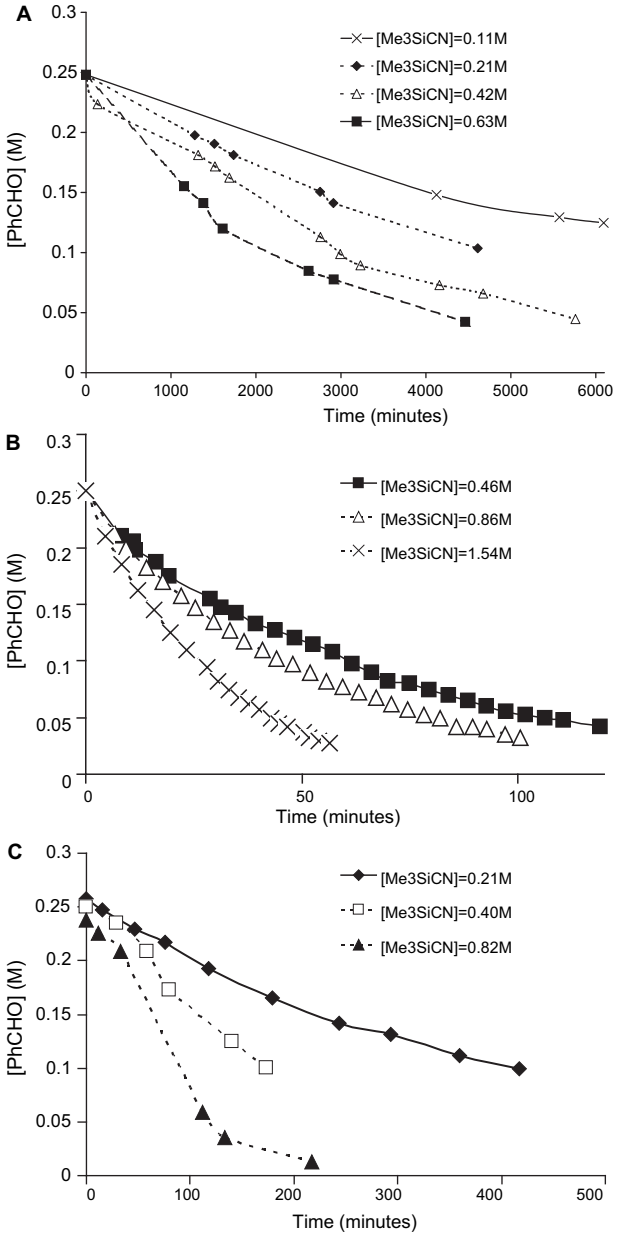

Figure 2. Demonstration that the rate of reactions catalysed by complexes **1**–**3** depends on the initial concentration of trimethylsilyl cyanide. (A) Catalyst **1**: [**1**]=0.025 M, [MePh$_2$PO]=0.093 M; (B) Catalyst **2**: [**2**]=0.005 M, [MePh$_2$PO]=0.035 M; (C) Catalyst **3**: [**3**]=0.005 M, [Ph$_3$PO]=0.025 M.

$$\text{Rate} = k_{\text{obs}}[\text{Me}_3\text{SiCN}] \quad \text{where } k_{\text{obs}}k[\text{catalyst}]^a[\text{R}_3\text{PO}]^b \tag{1}$$

$$\text{so } \log(k_{\text{obs}}) = \log(k) + a\log([\text{catalyst}]) + \text{blog}([\text{R}_3\text{PO}]) \tag{2}$$

The lack of dependence of the rate of reaction on the concentration of benzaldehyde can be interpreted in two ways:

1. The aldehyde is only involved in the mechanism after the rate determining step.
2. The catalytic cycle starts with rapid, reversible binding of the aldehyde to the catalyst, resulting in formation of a catalyst–aldehyde complex whose concentration remains constant throughout the reaction (saturation kinetics).

To distinguish between these two possibilities, NMR experiments were undertaken. For all three catalysts, the ^{1}H and ^{13}C NMR spectra of benzaldehyde (in deuterated dichloromethane for catalysts **1** and **3** and in deuterated toluene for catalyst **2**) showed no significant changes when equimolar amounts of catalyst or when equimolar amounts of catalyst and phosphine oxide were added. This strongly suggested that there was no significant formation of catalyst–aldehyde complexes. To investigate the possibility that the catalyst–aldehyde complexes only form in the presence of trimethylsilyl cyanide, reactions were carried out in the appropriate deuterated solvent using 10 mol % of each catalyst and a 10% excess of benzaldehyde relative to trimethylsilyl cyanide. Analysis of the reaction mixtures by ^{1}H NMR spectroscopy again provided no evidence for the presence of catalyst–aldehyde complexes. Thus, the kinetic data for all three catalysts was interpreted on the basis that the aldehyde is only involved in the mechanism after the rate determining step.

Having determined that all of the catalysts obey the same rate equation, the order with respect to both aluminium complex (Fig. 3) and phosphine oxide (Fig. 4) was determined for all three catalysts by varying the concentrations of these two components (Eq. 2). Figure 3 suggests that reactions catalysed by complexes **1** and **3** exhibit a first order dependence of the reaction rate on catalyst concentration. This was confirmed by a plot of [cat] against k_{obs} which in both cases gave a straight line passing through the origin. For catalyst **2** however, the order with respect to catalyst concentration was found to be ca. 0.5. Najera has shown[19] that the asymmetric addition of trimethylsilyl cyanide to aldehydes catalysed by complex **2**/triphenylphosphine oxide does not show a non-linear effect.[49] In contrast, the addition of other cyanide sources to aldehydes catalysed by complex **2** in the absence of triphenylphosphine oxide does display a non-linear effect.[20,22] This suggests that in the absence of phosphine oxide, complex **2** forms aggregates in solution and that one role of the triphenylphosphine oxide is to dissociate these aggregates. We have previously shown as part of a study of other catalyst systems,[42] that the observation of an order with respect to catalyst concentration of 0.5 is entirely consistent with a model in which the precatalyst is associated into dimers or higher species, but the catalytically active species is monomeric.

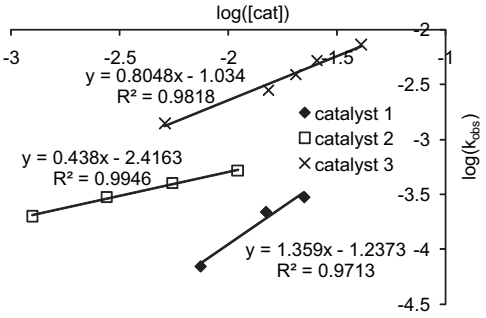

Figure 3. Determination of the order with respect to catalyst concentration for complexes **1**–**3**.

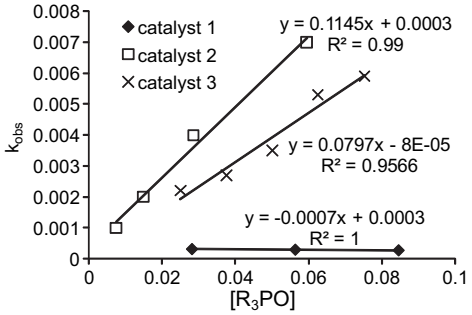

Figure 4. Determination of the order with respect to phosphine oxide concentration for complexes **1**–**3**. k_{obs} data for catalyst **2** have been multiplied by 10 to allow all the data to be plotted on the same scales.

Figure 4 shows that whilst reactions catalysed by complexes **2** and **3** were first order in phosphine oxide concentration, that catalysed by complex **1** was zero order in phosphine oxide concentration. Shibasaki has previously reported preliminary kinetic data showing that the rate of reaction decreases in the presence of phosphine oxide.[12,13] This is consistent with our own preliminary data reported in Table 1. However, the effect of varying the catalyst to phosphine oxide ratio had not previously been reported. In all of these reactions however, an excess (2–5 equiv) of phosphine oxide with respect to binol–aluminium complex was employed. Thus, the simplest explanation for the observed zero-order dependence is that one equivalent of phosphine oxide is required to bind to the aluminium of the active catalyst, changing its geometry to trigonal bipyramidal as previously reported, and that the phosphine oxide has no other role to play in the mechanism.

In contrast, the first order dependence on phosphine oxide concentration observed for catalysts **2** and **3** (using 2–15 equiv of phosphine oxide with respect to binol–aluminium complex in the case of complex **2** and 10–30 equiv of phosphine oxide with respect to aluminium(salen) complex in the case of complex **3**) suggests that the phosphine oxide has a second role in addition to coordination to the aluminium of the catalyst. The most obvious such role is to react with the trimethylsilyl cyanide as previously reported by Corey.[50,51] The different kinetic behaviour of complex **1** can then be accounted for by its internal phosphine oxides fulfilling this role. In the case of catalyst **2**, it should be noted however, that whilst this analysis may be valid for the homogeneous conditions employed in this work to study the kinetics, the optimised conditions developed by Najera involved the addition of 4 Å molecular sieves to the reaction and it was shown that under these conditions the active cyanating agent was hydrogen cyanide rather than trimethylsilyl cyanide.[18,19]

The full rate equations for catalysts **1**–**3** are summarised in Eqs. 3–5.

$$\text{Catalyst } \mathbf{1} : \text{rate} = k[\mathbf{1}][Me_3SiCN] \quad (3)$$

$$\text{Catalyst } \mathbf{2} : \text{rate} = k[\mathbf{2}]^{0.5}[MePh_2PO][Me_3SiCN] \quad (4)$$

$$\text{Catalyst } \mathbf{3} : \text{rate} = k[\mathbf{3}][Ph_3PO][Me_3SiCN] \quad (5)$$

To further investigate kinetic similarities and differences between catalysts **1**–**3** a variable temperature kinetics study was carried out to allow the activation parameters to be determined. Figure 5 shows the Arhenius plot for all three catalysts and the resulting activation enthalpies, entropies and Gibbs energies are given in Table 2, along with those of related titanium and vanadium

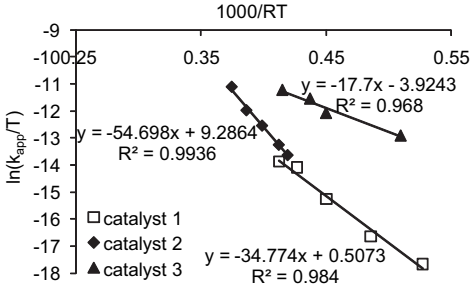

Figure 5. Arhenius plots for complexes **1**–**3**. Catalyst **1**: [**1**]=0.022 M, [$MePh_2$-PO]=0.084 M. Catalyst **2**: [**2**]=0.0027 M, [$MePh_2PO$]=0.015 M. Catalyst **3**: [**3**]=0.005 M, [Ph_3PO]=0.025 M.

Table 2
Activation parameters[a] for catalysts **1**–**3** and **9**–**12**

Catalyst	$\Delta H^{\ddagger}$ (kJ mol^{-1})	$\Delta S^{\ddagger}$ (J mol^{-1})	$\Delta G^{\ddagger}$ (kJ mol^{-1})[b]
1	34.8 (±1.1)	−162 (±5)	79.0 (±1.1)
2	54.7 (±2.7)	−61 (±9)	71.3 (±2.7)
3	17.7 (±1.3)	−155 (±5)	60.0 (±1.3)
9	35.9 (±3.2)	−86 (±12)	59.4 (±3.2)
10	27.6 (±4.9)	−184 (±17)	77.8 (±4.9)
11	32.5 (±3.2)	−125 (±12)	66.6 (±3.2)
12	20.4 (±2.9)	−136 (±10)	57.5 (±2.9)

[a] Error limits are calculated on the basis of a ±6% error in all of the rate data used to construct Figure 5.
[b] At 273 K.

based salen complexes **9**–**12** determined previously.[48] The overall trend in Gibbs energies of activations matches the observed catalytic activities of the complexes, with complexes **9** and **12** being the most active (reactions complete in 1–2 h at 0.1 mol% catalyst loading) and complexes **1** and **2** being least active (reactions require 10 mol% catalyst for 6–36 h).

Comparison of the data for catalysts **1** and **2** shows that they have similar Gibbs energies of activation (79 and 71 kJ mol^{-1}, respectively), but that this is made up of very different contributions from the enthalpies and entropies of activation. Catalyst **1** has a very negative entropy of activation, suggesting that it has a very highly ordered transition state. In contrast, catalyst **2** has the least negative entropy of activation of any of the catalysts (−61 J mol^{-1} compared to −162 J mol^{-1} for catalyst **1**). The significantly lower entropy of activation of complex **2** compared to complex **1** is consistent with deoligomerization of the precatalyst offsetting the entropic cost of bringing the various reaction components together. In contrast, catalyst **2** has the highest enthalpy of activation of any of the catalysts (55 kJ mol^{-1}) and this is 20 kJ mol^{-1} greater than the enthalpy of activation of catalyst **1**. This suggests that the diethylamino groups in catalyst **2** are not as effective Lewis bases as the phosphine oxide groups in catalyst **1**. However, it is known that under the optimal synthetic conditions (involving addition of 4 Å molecular sieves), the active cyanating agent in reactions catalysed by complex **2** is hydrogen cyanide rather than trimethylsilyl cyanide.[18,19] Under these conditions, the diethylamino groups would be expected to act as more effective Brønsted bases, thus accounting for the enhanced activity of catalyst **2** under the optimal conditions.

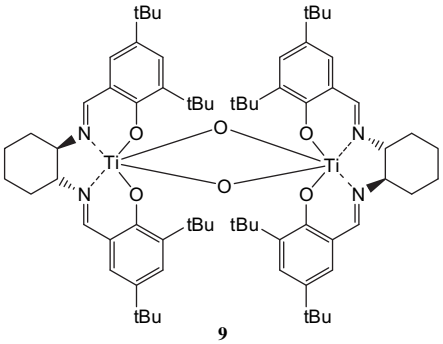

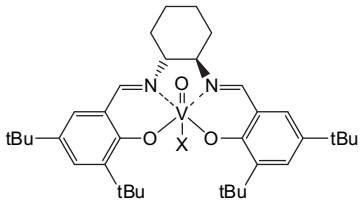

The data for catalyst **3** show that it has a very low enthalpy of activation compared to any of the other aluminium or salen based catalysts. Its entropy of activation is however more negative than any of the other salen based catalysts, except for complex **10**, which is known to be a very slow catalyst. This is consistent with reactions involving complex **3** requiring the presence of triphenylphosphine oxide as a Lewis base, whilst reactions catalysed by complexes **9**–**12** do not require the addition of a separate Lewis base. Thus, in the case of reactions catalysed by complex **3** more components have to be brought together in the transition state resulting in a more negative entropy of activation, which largely offsets its very low enthalpy of activation. The overall result is that complex **3** is a less active catalyst than the two very highly active catalysts (**9** and **12**), but more active than any of the other catalysts.

3. Mechanistic analysis

The catalytic cycle previously proposed by Shibasaki[13] to account for catalysis by complex (*S*)-**1** is shown in Scheme 4. This mechanism is consistent with the zero-order dependence on phosphine oxide concentration and the first order dependence on catalyst concentration determined by our kinetics results. However, benzaldehyde is involved in the catalytic cycle (step A) before trimethylsilyl cyanide is involved (step B). Since NMR experiments showed no evidence for the formation of a significant concentration of a species such as **14**, this is inconsistent with the kinetic data, which show the reaction to be first order in trimethylsilyl cyanide concentration and zero order in benzaldehyde concentration.

To make the catalytic cycle shown in Scheme 4 consistent with the kinetic data, all, that is, required is that steps A and B be interchanged so that the in situ assembled catalyst **13** reacts first (in the rate determining step) with trimethylsilyl cyanide and subsequently with benzaldehyde.

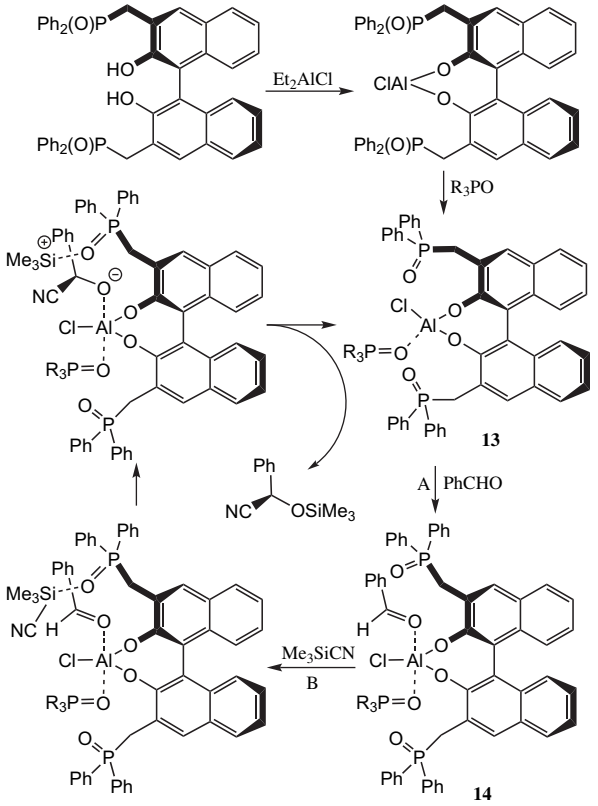

Scheme 4. Catalytic cycle for complex **1**.

The catalytic cycle proposed by Najera to account for catalysis by complex (*S*)-**2** is shown in Scheme 5. However, this catalytic cycle is for reactions carried out in the presence of 4 Å molecular sieves to generate hydrogen cyanide in situ. Therefore, our kinetic results will not be directly applicable to this catalytic cycle. It seems likely, that in the absence of a water source, the actual catalytic cycle involving catalyst **2** will resemble that shown in Scheme 4 for Shibasaki's catalyst, but with external phosphine oxide activating the cyanide[50,51] (Scheme 6). This would account for the first order dependence of the rate of reaction on phosphine oxide concentration observed with complex **2**, and provided the formation of complex **17** was rate determining would also be consistent with the zero-order dependence of the rate on the benzaldehyde concentration.

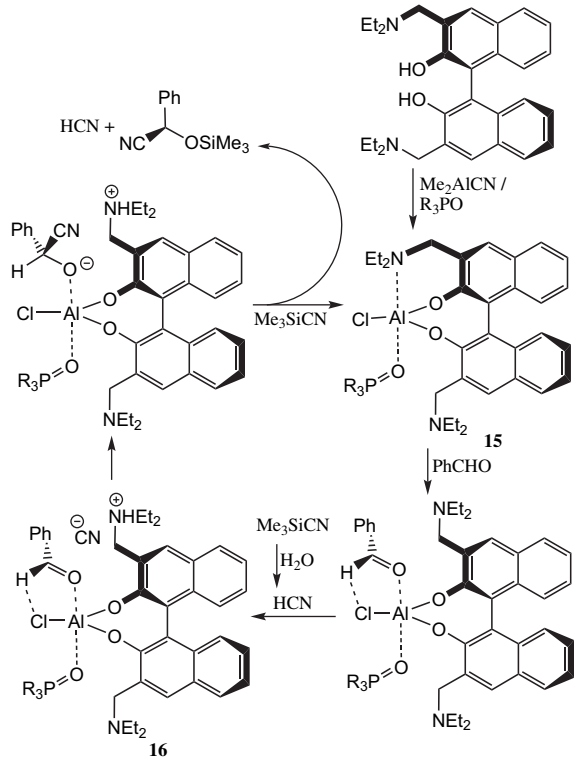

Scheme 5. Catalytic cycle for complex **2** in the presence of 4 Å molecular sieves.

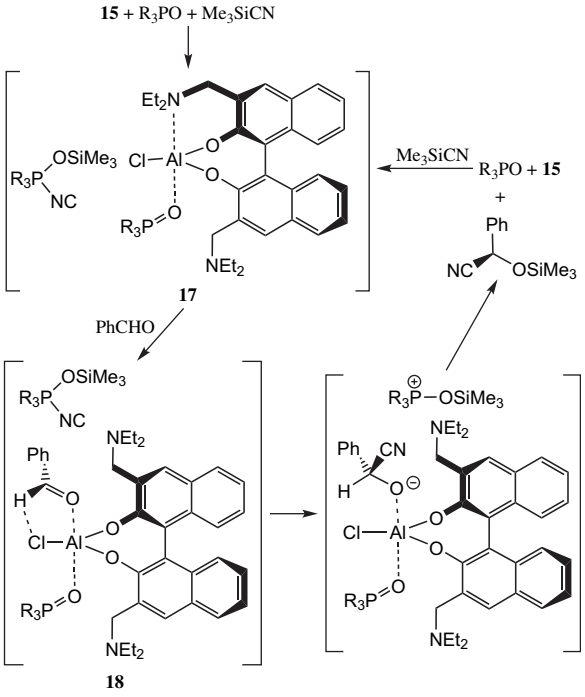

Scheme 6. Catalytic cycle for complex **2** in the absence of 4 Å molecular sieves.

Stereochemically, the mechanism shown in Scheme 5 involves the addition of cyanide to the *si*-face of the coordinated benzaldehyde within complex **16**. However, the *si*-face of the aldehyde in complex **16** (and the analogous complex **18** in Scheme 6) also appears to be the less hindered face for intermolecular addition to occur on. Therefore, addition of cyanide to complex **18** would also be expected to occur on the *si*-face of the coordinated aldehyde, leading to the same stereochemical outcome ((*R*)-cyanohydrin from (*S*)-catalyst) as that predicted by Scheme 5. This analysis was supported by results reported by Najera using the aluminium complex **19** of binol.[19] Under a range of conditions, (*S*)-**19** catalysed the asymmetric synthesis of (*R*)-mandelonitrile trimethylsilyl ether, derived by addition of cyanide to the *si*-face of benzaldehyde.

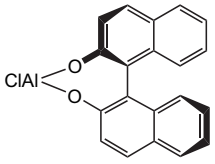

19

The order of 0.5 observed for the dependence of the rate on catalyst concentration for complex **2** is consistent with previous results reported by Najera. Thus, whilst the asymmetric addition of trimethylsilyl cyanide to aldehydes carried out in the presence of a phosphine oxide co-catalyst was found to show a linear relationship between the enantiomeric excess of the catalyst and the enantiomeric excess of the product,[19] the asymmetric addition of cyanoformates[23] or cyanophosphonates[20,22] to aldehydes which occur in the absence of a phosphine oxide co-catalyst show a pronounced non-linear relationship.[49] This indicates that complex **2** exists in toluene solution in equilibrium with oligomeric species, but that these oligomers are completely broken down to mononuclear complex **15** in the presence of a phosphine oxide co-catalyst. Thus, multiple catalytically active species **15** are obtained from each initially oligomeric complex **2**. The same effect also explains the remarkably small negative entropy of activation observed for complex **2** (Table 2), since the coming together of multiple molecules required to assemble the catalytically active species in Schemes 5 and 6 is offset by the dissociation of the initially oligomeric complex.

The kinetic data for complex **3** support a mechanism such as that shown in Scheme 7, which we have previously proposed for asymmetric cyanohydrin synthesis catalysed by complex **3** in the presence of a phosphine oxide co-catalyst.[29] This involves the use of triphenylphosphine oxide to activate the trimethylsilyl cyanide[50,51] and complexation of the resulting species to one of the aluminium ions of complex **3** in the rate determining step of the catalytic cycle, thus explaining the first order dependence of the rate of reaction on the concentrations of catalyst, phosphine oxide and trimethylsilyl cyanide. Coordination of benzaldehyde to the other aluminium ion occurs after the rate determining step, and subsequent intramolecular transfer of cyanide to the *si*-face of the coordinated aldehyde (for reactions involving catalyst **3** derived from (*S*,*S*)-diaminocyclohexane) leads to the formation of (*R*)-cyanohydrin trimethylsilyl ethers after silylation of the initially formed aluminium coordinated cyanohydrin.

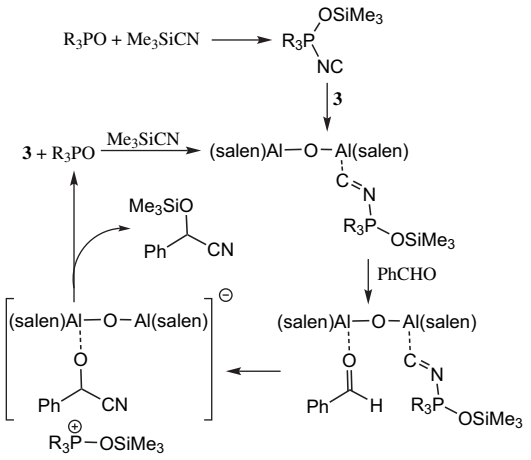

Scheme 7. Catalytic cycle for complex **3**.

4. Application to magnesium-based catalyst system

In 1993, Corey reported a unique magnesium-based catalyst system for asymmetric cyanohydrin synthesis.[52] Bisoxazoline–magnesium complex **20** was used as a chiral Lewis acid along with bisoxazoline **21** as a chiral Lewis base to catalyse the asymmetric addition of trimethylsilyl cyanide to aldehydes. To demonstrate that the mechanistic analysis developed in this work had applicability beyond aluminium complexes, it was decided to carry out a kinetic analysis of asymmetric cyanohydrin synthesis catalysed by complex **20**.

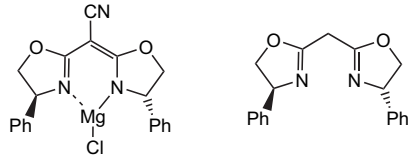

20 **21**

Initial studies showed that the system developed by Corey was not amenable to kinetic analysis. Trial reactions were initially carried out at −78 °C under the optimal conditions reported by Corey (20 mol % **20** and 12 mol % **21**). Unfortunately, manual sampling of the reaction mixture was not possible as reaction occurred during the sampling process. Monitoring of the kinetics by ^{1}H NMR spectroscopy was also not possible due to the mixed solvent system of dichloromethane and propionitrile necessary to dissolve catalysts **20** and **21**. Attempts to carry out kinetic analyses at a higher temperature (0 °C) also failed as the catalyst system decomposed during the reaction under these conditions.

To avoid these problems, a new catalytic system was developed in which magnesium complex **20** was used as the chiral Lewis acid in conjunction with methyldiphenylphosphine oxide as an achiral Lewis base. This combination of catalysts was soluble in dichloromethane, and at 25 °C the combination of (*S*,*S*)-**20** (2 mol %) and methyldiphenylphosphine oxide (8 mol %) catalysed the asymmetric addition of trimethylsilyl cyanide to benzaldehyde with 100% conversion after 16 h, to giving (*S*)-mandelonitrile trimethylsilyl ether with 35% enantiomeric excess. Reactions carried out in deuterated dichloromethane could be monitored by ^{1}H NMR spectroscopy.

This catalyst system was again found to show overall first order kinetics (Fig. 6), and reactions carried out at four different trimethylsilyl cyanide concentrations confirmed that the reactions were first order in trimethylsilyl cyanide concentration (Fig. 7). Reactions carried out at various concentrations of complex **20** (Fig. 8) and methyldiphenylphosphine oxide (Fig. 9) also showed that the reaction was first order in both catalyst components. Thus, the full rate equation for reactions catalysed by complex **20** is:

$$\text{rate} = k[\mathbf{20}][\text{MePh}_2\text{PO}][\text{Me}_3\text{SiCN}] \quad (6)$$

This is the same rate equation as that determined for reactions catalysed by complex **3** (Eq. 5) and is consistent with a mechanism such as that shown in Scheme 8 in which the formation of complex

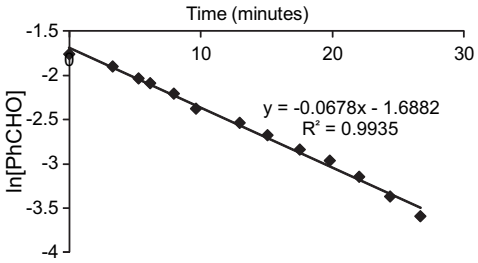

Figure 6. First order kinetics plots for catalyst **20** ([PhCHO]$_0$=0.17 M, [Me$_3$SiCN]$_0$=0.17 M, [**20**]=3.46 mM, [MePh$_2$PO]=3.44 mM).

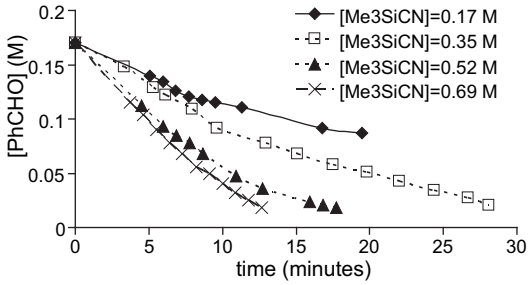

Figure 7. Demonstration that the rate of reactions catalysed by complex **20** depends on the initial concentration of trimethylsilyl cyanide ([PhCHO]$_0$=0.17 M, [**20**]=3.46 mM, [MePh$_2$PO]=3.44 mM).

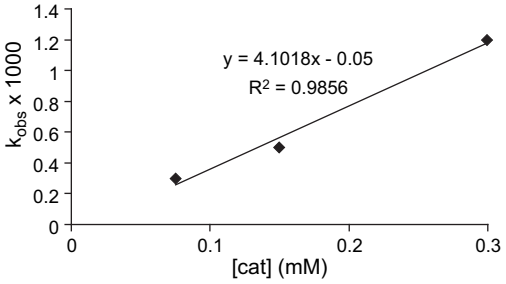

Figure 8. Determination of the order with respect to catalyst **20** concentration ([PhCHO]$_0$=0.17 M, [Me$_3$SiCN]$_0$=0.17 M, [MePh$_2$PO]=3.44 mM).

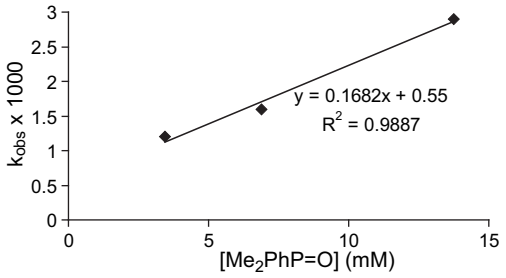

Figure 9. Determination of the order with respect to phosphine oxide concentration for reactions catalysed by complex **20** ([PhCHO]$_0$=0.17 M, [Me$_3$SiCN]$_0$=0.17 M, [**20**]=3.46 mM).

22 is rate determining, which is closely analogous to the catalytic cycle for catalyst **3** (Scheme 7). The mechanism shown in Scheme 8 is different to that proposed by Corey[52] for the **20**/**21** catalyst system, but this reflects the fact that methyldiphenylphosphine oxide is a Lewis base, which can activate trimethylsilyl cyanide,[50,51] whilst bisoxazoline **21** could function as a Brønsted base to activate hydrogen cyanide generated in situ from trimethylsilyl cyanide.

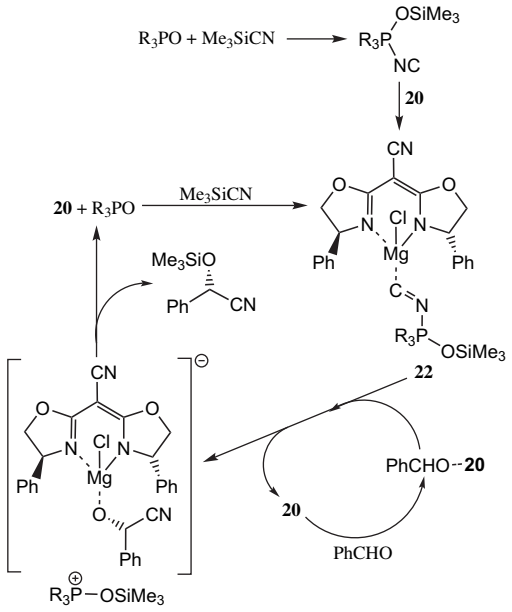

Scheme 8. Catalytic cycle for complex **20** and $MePh_2PO$.

5. Conclusions

Although the rate equations for catalysts **1**–**3** and **20** differ in detail, they are consistent with a common mechanistic basis for asymmetric cyanohydrin synthesis. This involves activation of the aldehyde by a Lewis acid and activation of the trimethylsilyl cyanide by a Lewis base. When a proton source is present in the reaction mixture, the trimethylsilyl cyanide may be hydrolysed to hydrogen cyanide, which can be activated by a Brønsted base rather than a Lewis base. This dual activation of both components of the reaction can be achieved by a single catalytic entity comprising both Lewis acidic and basic sites or by two different catalytic species and appears to be a general feature of the most effective catalysts for asymmetric cyanohydrin synthesis.[1–3] When the Lewis acid and base are in separate molecules, the Lewis acid is usually the source of chirality within the catalytic assembly as it will be directly coordinated to the prochiral aldehyde, though examples are known where both the Lewis acid and the base are chiral species.[52] Since simultaneous catalysis by Lewis acids and Lewis bases can be applied to reactions other than cyanohydrin synthesis,[53] the results of this study may also have wider generality.

6. Experimental

6.1. Instrumentation and general methods

CH_2Cl_2 was dried by distillation from CaH_2. All deuterated solvents were purchased from GOSS chemicals. Chromatographic separations were performed with silica gel 60 (230–400 mesh). All UV spectra were recorded on a Biochrom Libra S12 spectrometer (100–240 V). ^{1}H NMR spectra were recorded on Bruker Avance 300, Jeol ECS 400 or Jeol Lambda 500 MHz spectrometers at the temperatures specified. Chiral GC analysis was carried out on a Varian 450GC using a Supelco Gamma DEX 120 fused silica capillary column (30 m×0.25 mm) with hydrogen as a carrier gas (flow rate 2.0 mL/min, column pressure 10 psi). Initial temperature 95 °C, final temperature 180 °C, ramp rate 5.0 °C/min.

6.2. BINOLAM 6[54,55]

A solution of *s*-BuLi (1.8 mL of a 1.3 M solution in hexanes) was added dropwise over 15 min to a stirred solution of 2,2′-bis(*N*,*N*-diethylcarbamoyloxy)-1,1′-binaphthyl[39] **4** (500 mg, 1.3 mmol) and TMEDA (0.31 mL, 2.1 mmol) in dry THF (10 mL) at −78 °C under nitrogen. The reaction was kept at −78 °C for one hour, then allowed to warm to room temperature and stir overnight. The mixture was quenched with NH_4Cl and the product extracted with CH_2Cl_2 (3×50 mL). The combined organic phases were washed with brine, dried ($MgSO_4$) and the solvent evaporated to leave bisamide **5**, which was used without further purification.

To a solution of the above prepared compound **5** in THF (20 mL) at 0 °C was added $LiAlH_4$ (116 mg, 3.0 mmol). The reaction was then heated to reflux overnight, quenched with a saturated KF solution (1 mL), filtered through Celite® and the solvent evaporated. The residue was extracted with CH_2Cl_2, washed with phosphate buffer and brine and the organic layer dried ($MgSO_4$) and concentrated to leave a yellow oil, which was purified by column chromatography ($CHCl_3$/MeOH, 25:1) to give BINOLAM **6** as a pale yellow solid (205 mg, 63% from **4**). Mp 140–141 °C (lit.[54] 138–139 °C); $[\alpha]_D^{20}$ +147.6 (*c* 0.5, $CHCl_3$) (lit.[55] +147 (*c* 0.5, $CHCl_3$)); δ_H($CDCl_3$) 1.01 (12H, t *J* 7.2 Hz, CH_3), 2.59 (8H, q *J* 7.2 Hz, NCH_2CH_3), 3.85 (2H, d *J* 13.5 Hz, $ArCH_2$), 4.13 (2H, d, *J* 13.5 Hz, $ArCH_2$), 7.1–7.3 (6H, m, ArH), 7.68 (2H, s, ArH), 7.78 (2H, d *J* 7.8 Hz, ArH).

6.3. *O*-Trimethylsilyl mandelonitrile using catalyst 1

To a solution of the substituted binol ligand (13 mg, 0.0182 mmol) in dry CH_2Cl_2 (1 mL) under nitrogen, was added Me_2AlCl (18 μL, 0.018 mmol, 1.0 M solution in hexanes). The resulting mixture was cooled to −40 °C, then benzaldehyde (21 mg, 0.192 mmol) and Me_3SiCN (34 mg, 0.345 mmol) were added and the reaction stirred at −40 °C for 36 h. The solution was then filtered and evaporated. A sample was analysed by ^{1}H NMR spectroscopy to determine the conversion. To the rest of the residue, acetonitrile (1 mL), a few drops of Ac_2O and a catalytic amount of $Sc(OTf)_3$ were added and the mixture stirred at room temperature for five minutes. The reaction was filtered through SiO_2 and analysed by chiral GC to determine the enantioselectivity.

6.4. *O*-Trimethylsilyl mandelonitrile using catalyst 2

To a suspension of (*R*)-BINOLAM **6** (11.4 mg, 0.025 mmol), Ph_3PO (28 mg, 0.1 mmol) and 4 Å molecular sieves (62 mg) in dry toluene (1 mL) under nitrogen, was added Me_2AlCl (25 μL, 0.025 mmol, 1.0 M solution in hexanes). The resulting mixture was cooled to −20 °C, then benzaldehyde (27 mg, 0.25 mmol) and Me_3SiCN (100 μL, 0.75 mmol) were added and the reaction stirred at −20 °C for six hours. The solution was then filtered and evaporated. A sample was analysed by ^{1}H NMR spectroscopy to determine the conversion. To the rest of the residue, acetonitrile (1 mL), a few drops of Ac_2O and a catalytic amount of $Sc(OTf)_3$ were added and the mixture stirred at room temperature for five minutes. The reaction was filtered through SiO_2 and analysed by chiral GC to determine the enantioselectivity.

6.5. *O*-Trimethylsilyl mandelonitrile using catalyst 3

Complex **3** (11 mg, 0.0095 mmol) and Ph_3PO (13 mg, 0.047 mmol) were dissolved in CH_2Cl_2 (1 mL). Benzaldehyde (51 mg, 0.48 mmol)

was added and the solution cooled to −40 °C. Me_3SiCN (75 mg, 0.76 mmol) was then added and the solution stirred at −40 °C for 16 h. The solution was then passed through a short silica plug eluting with CH_2Cl_2. The eluent was evaporated in vacuo and the residue was analysed by ^1H NMR spectroscopy to determine the conversion. The residue was then dissolved in acetonitrile (1 mL), a few drops of Ac_2O and a catalytic amount of $Sc(OTf)_3$ were added and the mixture stirred at room temperature for 20 min. The reaction was filtered through SiO_2 and analysed by chiral GC to determine the enantioselectivity.

6.6. Kinetics study using catalyst 1

To a solution of the substituted binol ligand and methyldiphenylphosphine oxide in CD_2Cl_2 (0.75 mL), Me_2AlCl (1 equiv relative to the amount of ligand) was added under N_2 and the mixture stirred at room temperature for one hour. Then, benzaldehyde was added and the sample transferred to a NMR tube followed by the addition of Me_3SiCN. The reaction tube was immediately cooled with liquid N_2 and transferred to the NMR spectrometer. A ^1H NMR spectrum was then recorded at −40 °C at appropriate intervals (every few minutes) over a period of ca. two hours depending on the concentrations of the various components. The quantity of each reagent varied depending on the concentration required. To construct the Arhenius plot, the reaction temperature was varied between −40 and +20 °C.

6.7. Kinetics study using catalyst 2

To a solution of (*R*)-BINOLAM **6** and methyldiphenylphosphine oxide in toluene-d_8 (0.75 mL), was added Me_2AlCl under N_2 and the mixture stirred at RT for one hour. Then, benzaldehyde was added and the sample was transferred to a NMR tube followed by addition of Me_3SiCN. A ^1H NMR spectrum was then recorded at appropriate intervals (every few minutes) over a period of ca. four hours depending on the concentrations of the various components. The quantity of each reagent varied depending on the concentration required. To construct the Arhenius plot, the reaction temperature was varied between +20 and +55 °C.

6.8. Kinetics study using catalyst 3

Catalyst **3** and Ph_3PO were dissolved in freshly distilled CH_2Cl_2 (1.75 mL) and the solution cooled to 0 °C in an ice bath. A sample (0.50 μL) was removed and diluted into CH_2Cl_2 (3.0 mL) to be used as the reference sample to zero the spectrophotometer. Benzaldehyde was added to the reaction mixture and another sample (0.50 μL) removed and also diluted into CH_2Cl_2 (3.0 ml). The absorbance of the sample was measured at 246 nm to provide the t=0 reading. Me_3SiCN was added to the reaction mixture and the kinetics monitored by taking samples (0.50 μL) and quenching them into CH_2Cl_2 (3.0 ml) at appropriate time intervals over a period of ca. six hours depending on the concentrations of the various components. The quantity of each reagent varied depending on the concentration required. To construct an Arhenius plot, the reaction temperature was varied between −32 and+23 °C.

6.9. *O*-Trimethylsilyl mandelonitrile using catalyst 20

To a solution of cyanobox ligand[52] (1 mg, 0.003 mmol) in CH_2Cl_2 (2 mL) was added ^iPrMgCl (1.5 μL of a 2.0 M solution in Et_2O, 0.003 mmol) and the resulting solution was stirred at room temperature for one hour under a nitrogen atmosphere. Then, $MePh_2PO$ (2.6 mg, 0.012 mmol) was added, followed by benzaldehyde (0.015 mL, 0.15 mmol) and Me_3SiCN (0.02 mL, 0.30 mmol). The solution was then stirred for 16 h before being filtered and evaporated. A sample was analysed by ^1H NMR spectroscopy to determine the conversion. The residue was then dissolved in acetonitrile (1 mL), a few drops of Ac_2O and a catalytic amount of $Sc(OTf)_3$ were added and the mixture stirred at room temperature for 10 min. The reaction was filtered through SiO_2 and analysed by chiral GC to determine the enantioselectivity.

6.10. Kinetics study using catalyst 20

To a solution of cyanobox ligand[52] in CD_2Cl_2 (2 mL) was added ^iPrMgCl (2.0 M solution in Et_2O) and the resulting solution was stirred at room temperature for one hour under a nitrogen atmosphere. Then, $MePh_2PO$ was added, followed by benzaldehyde and Me_3SiCN. The solution was transferred to a NMR tube and a ^1H NMR spectrum was recorded every few minutes over a period of one hour depending on the concentrations of the various components.

References and notes

1. North, M.; Usanov, D. L.; Young, C. *Chem. Rev.* **2008**, *108*, 5146–5226.
2. Riant, O.; Hannedouche, J. *Org. Biomol. Chem.* **2007**, *5*, 873–888.
3. Davie, E. A. C.; Mennen, S. M.; Xu, Y.; Miller, S. J. *Chem. Rev.* **2007**, *107*, 5759–5812.
4. Malkov, A. V.; Kočovský, P. *Eur. J. Org. Chem.* **2007**, 29–36.
5. Purkarthofer, T.; Skranc, W.; Schuster, C.; Griengl, H. *Appl. Microbiol. Biotechnol.* **2007**, *76*, 309–320.
6. Blacker, A. J.; North, M.; Belokon, Y. N. *Chemistry Today* **2004**, *22*, 30–32 (Chiral Catalysis: C–C Coupling and Oxidation Supplement).
7. Blacker, J.; North, M. *Chem. Ind.* **2005**, 22–25.
8. Lapworth, A. *J. Chem. Soc.* **1903**, 995–1005.
9. Lapworth, A. *J. Chem. Soc.* **1904**, 1206–1214.
10. Lapworth, A.; Helmuth, R.; Manske, F. *J. Chem. Soc.* **1928**, 2533–2549.
11. Lapworth, A.; Helmuth, R.; Manske, F. *J. Chem. Soc.* **1930**, 1976–1981.
12. Hamashima, Y.; Sawada, D.; Kanai, M.; Shibasaki, M. *J. Am. Chem. Soc.* **1999**, *121*, 2641–2642.
13. Hamashima, Y.; Sawada, D.; Nogami, H.; Kanai, M.; Shibasaki, M. *Tetrahedron* **2001**, *57*, 805–814.
14. Sawada, D.; Shibasaki, M. *Angew. Chem., Int. Ed.* **2000**, *39*, 209–213.
15. Sawada, D.; Kanai, M.; Shibasaki, M. *J. Am. Chem. Soc.* **2000**, *122*, 10521–10532.
16. Takamura, M.; Yanagisawa, H.; Kanai, M.; Shibasaki, M. *Chem. Pharm. Bull.* **2002**, *50*, 1118–1121.
17. Nogami, H.; Kanai, M.; Shibasaki, M. *Chem. Pharm. Bull.* **2003**, *51*, 702–709.
18. Casas, J.; Nájera, C.; Sansano, J. M.; Saá, J. M. *Org. Lett.* **2002**, *4*, 2589–2592.
19. Casas, J.; Nájera, C.; Sansano, J. M.; Saá, J. M. *Tetrahedron* **2004**, *60*, 10487–10496.
20. Baeza, A.; Casas, J.; Nájera, C.; Sansano, J. M.; Saá, J. M. *Angew. Chem., Int. Ed.* **2003**, *42*, 3143–3146.
21. Casas, J.; Baeza, A.; Sansano, J. M.; Nájera, C.; Saá, J. M. *Tetrahedron: Asymmetry* **2003**, *14*, 197–200.
22. Baeza, A.; Nájera, C.; Sansano, J. M.; Saá, J. M. *Chem.—Eur. J.* **2005**, *11*, 3849–3862.
23. Baeza, A.; Casas, J.; Nájera, C.; Sansano, J. M.; Saá, J. M. *Eur. J. Org. Chem.* **2006**, 1949–1958.
24. Baeza, A.; Casas, J.; Nájera, C.; Saá, J. M. *J. Org. Chem.* **2006**, *71*, 3837–3848.
25. Baeza, A.; Nájera, C.; Sansano, J. M. *Eur. J. Org. Chem.* **2007**, 1101–1112.
26. Baeza, A.; Sansano, J. M.; Saá, J. M.; Nájera, C. *Pure Appl. Chem.* **2007**, *79*, 213–221.
27. Qin, Y.-C.; Liu, L.; Pu, L. *Org. Lett.* **2005**, *7*, 2381–2383.
28. Qin, Y.-C.; Liu, L.; Sabat, M.; Pu, L. *Tetrahedron* **2006**, *62*, 9335–9348.
29. North, M.; Williamson, C. *Tetrahedron Lett.* **2009**, *50*, 3249–3252.
30. Kim, S. S.; Song, D. H. *Eur. J. Org. Chem.* **2005**, 1777–1780.
31. Kim, S. S. *Pure Appl. Chem.* **2006**, *78*, 977–983.
32. Kim, S. S.; Kwak, J. M. *Tetrahedron* **2006**, *62*, 49–53.
33. Zeng, Z.; Zhao, G.; Zhou, Z.; Tang, C. *Eur. J. Org. Chem.* **2008**, 1615–1618.
34. Chen, F.-X.; Zhou, H.; Liu, X.; Qin, B.; Feng, X.; Zhang, G.; Jiang, Y. *Chem.—Eur. J.* **2004**, *10*, 4790–4797.
35. Alaaeddine, A.; Roisnel, T.; Thomas, C. M.; Carpentier, J.-F. *Adv. Synth. Catal.* **2008**, *350*, 731–740.
36. Nicewicz, D. A.; Yates, C. M.; Johnson, J. S. *Angew. Chem., Int. Ed.* **2004**, *43*, 2652–2655.
37. Nicewicz, D. A.; Yates, C. M.; Johnson, J. S. *J. Org. Chem.* **2004**, *69*, 6548–6555.
38. Meléndez, J.; North, M.; Pasquale, R. *Eur. J. Inorg. Chem.* **2007**, 3323–3326.
39. Dennis, M. R.; Woodward, S. *J. Chem. Soc., Perkin Trans. 1* **1998**, 1081–1085.
40. Norsikian, S.; Holmes, I.; Lagasse, F.; Kagan, H. B. *Tetrahedron Lett.* **2002**, *43*, 5715–5717.
41. Belokon, Y. N.; Caveda-Cepas, S.; Green, B.; Ikonnikov, N. S.; Khrustalev, V. N.; Larichev, V. S.; Moscalenko, M. A.; North, M.; Orizu, C.; Tararov, V. I.; Tasinazzo, M.; Timofeeva, G. I.; Yashkina, L. V. *J. Am. Chem. Soc.* **1999**, *121*, 3968–3973.
42. Belokon, Y. N.; Green, B.; Ikonnikov, N. S.; Larichev, V. S.; Lokshin, B. V.; Moscalenko, M. A.; North, M.; Orizu, C.; Peregudov, A. S.; Timofeeva, G. I. *Eur. J. Org. Chem.* **2000**, 2655–2661.
43. Belokon, Y. N.; North, M.; Parsons, T. *Org. Lett.* **2000**, *2*, 1617–1619.
44. Belokon, Y. N.; Green, B.; Ikonnikov, N. S.; North, M.; Parsons, T.; Tararov, V. I. *Tetrahedron* **2001**, *57*, 771–779.

45. Belokon, Y. N.; Clegg, W.; Harrington, R. W.; Young, C.; North, M. *Tetrahedron* **2007**, *63*, 5287–5299.
46. Belokon, Y. N.; Maleev, V. I.; North, M.; Usanov, D. L. *Chem. Commun.* **2006**, 4614–4616.
47. Belokon, Y. N.; Clegg, W.; Harrington, R. W.; North, M.; Young, C. *Inorg. Chem.* **2008**, *47*, 3801–3814.
48. Belokon, Y. N.; Clegg, W.; Harrington, R. W.; Maleev, V. I.; North, M.; Omedes Pujol, M.; Usanov, D. L.; Young, C. *Chem.—Eur. J.* **2009**, *15*, 2148–2165.
49. Satyanarayana, T.; Abraham, S.; Kagan, H. B. *Angew. Chem., Int. Ed.* **2009**, *48*, 456–494.
50. Ryu, D. H.; Corey, E. J. *J. Am. Chem. Soc.* **2004**, *126*, 8106–8107.
51. Ryu, D. H.; Corey, E. J. *J. Am. Chem. Soc.* **2005**, *127*, 5384–5387.
52. Corey, E. J.; Wang, Z. *Tetrahedron Lett.* **1993**, *34*, 4001–4004.
53. Ma, J.-A.; Cahard, D. *Angew. Chem., Int. Ed.* **2004**, *43*, 4566–4583.
54. Saá, J. M.; Tur, F.; González, J.; Vega, M. *Tetrahedron: Asymmetry* **2006**, *17*, 99–106.
55. Kitajima, H.; Ito, K.; Katsuki, T. *Tetrahedron* **1997**, *53*, 17015–17028.